Contemporary Mathematics
http://ojs.wiserpub.com/index.php/CM/

Research Article

Impact of First Order Slip Condition on Peristaltic Transport of a Pseudoplastic Fluid Under MHD Effect Bounded by Permeable Walls with Suction and Injection

S. Sivaranjani, A. Kavitha*

Department of Mathematics, School of Advanced Sciences, Vellore Institute of Technology, Vellore, 632014, India
E-mail: kavitha@vit.ac.in

Received: 25 September 2024; **Revised:** 9 January 2025; **Accepted:** 10 January 2025

Abstract: This research investigates the impact of first-order slip conditions on the peristaltic flow of a pseudoplastic fluid in the presence of a magnetic field, taking into the effects of suction and injection. Pseudoplastic fluids, which are shear-thinning, undergo a reduction in viscosity as shear rate increases, as opposed to Newtonian fluids, which maintain a constant viscosity regardless of applied shear stress. This characteristic is commonly found in fluids such as blood, polymer solutions, and certain industrial slurries, making them well-suited for applications where efficient flow under stress is critical. The analytical solution for frictional force and pressure rise was derived using perturbation techniques, assuming a long wavelength and low Reynolds number. Matrix Laboratory (MATLAB) simulations provided visual insights into how key parameters such as the magnetic field strength M, the slip parameter α, and the suction and injection parameter k influence velocity profiles, pressure distribution, and friction forces. The findings indicate that a magnetic field M increases the fluid's pumping efficiency, while a higher slip parameter α enhances the perturbation parameter Γ. Additionally, increasing the suction and injection parameters improves the overall pressure gradient, leading to more effective fluid transport across the system.

***Keywords*:** shear-thinning behavior, suction and injection, peristaltic transport, magnetohydrodynamic (MHD)

MSC: 76A05, 76D07, 76M99, 76W05

Symbols and abbreviations

b	Amplitude
ϕ	Amplitude ratio
α	Slip parameter
a	Half width of the channel
P	Pressure
M	Magnetic parameter
Re	Reynolds number
S_{xx}, S_{xy}, S_{yy}	Stress component

DOI: https://doi.org/10.37256/cm.6120255786

k	Suction/injection parameter
Γ	Perturbation parameter
t	Time
v_0	Velocity
$(\bar{U}, \bar{V})$	Velocity components in lab frame
$(\bar{u}, \bar{v})$	Velocity components in wave frame
μ	Viscosity
δ	Wave
λ	Wavelength
c	Wavespeed

1. Introduction

Peristaltic transport, a mechanism where fluid is propelled through a channel by progressive wave-like contractions along the walls, plays a critical role in both biomedical and industrial processes. The dynamics of this transport become more intricate when considering pseudoplastic (shear-thinning) fluids, such as biological fluids or polymer solutions, due to their non-Newtonian nature. Furthermore, the presence of a first-order partial slip condition at the walls significantly impacts flow characteristics.

The introduction of permeable walls with suction and injection adds another layer of complexity. Suction and injection are often used to control fluid influx and outflux in channels, which is vital for regulating flow rate and pressure in applications like dialysis or industrial filtration systems. Together, these factors-pseudoplasticity, MHD effects, partial slip, and wall permeability with suction/injection-create a complex interplay that directly impacts the efficiency of peristaltic transport systems.

Ali et al. [1] explored the effects of rotational forces on peristaltic flow for pseudoplastic fluids, demonstrating how rotation influences the velocity and pressure distributions in a wavy channel. While their study focuses on rotational effects, our study builds upon similar fluid dynamics principles but focuses specifically on the impact of first-order partial slip conditions on peristaltic transport. The results of our study provide further insight into how boundary slip conditions, rather than rotational forces, can alter the flow behavior and pressure drop in pseudoplastic fluids.

Ramesh et al. [2] explored the MHD peristaltic flow of pseudoplastic fluids in a vertical asymmetric channel with a porous substrate, incorporating heat and mass transfer effects. They examined the complexities induced by the porous medium and shear-thinning fluid behavior. In this study, however, also considers MHD effects but in a simpler straight channel configuration, focusing on the impact of first-order slip conditions rather than porous media. This contrast highlights how different channel geometries and boundary conditions affect fluid dynamics in MHD peristaltic transport.

Noreen et al. [3] examined the combined effects of peristaltic and electroosmotic pumping in pseudoplastic fluids. Their work emphasized how these two pumping mechanisms influence fluid behavior in a non-Newtonian fluid. Unlike their focus on electroosmotic effects, In this paper concentrates on MHD peristaltic flow and the impact of boundary slip. While both studies investigate non-Newtonian fluid flow, we delve deeper into the effects of slip conditions in an MHD framework, which is absent in Noreen et al.'s research.

Jayavel et al. [4] focused on electroosmotic flow of pseudoplastic nanofluids under peristaltic pumping, exploring the combined effects of electrokinetic forces, fluid rheology, and wall characteristics. Their study is particularly relevant to microfluidic applications and biomedical devices. In this study diverges by examining MHD effects and first-order slip conditions on pseudoplastic fluid flow, without considering electroosmotic forces. This difference marks our work as more focused on the magnetohydrodynamic aspects of peristaltic flow, with implications for fields like drug delivery and filtration systems.

Akhtar et al. [5] investigated the peristaltic flow of a Rabinowitsch fluid in an elliptical duct, focusing on thickening and shear-thinning behaviors and the effects of duct shape and heating. Their use of special polynomials to solve the governing equations contrasts with our analytical approach, which uses perturbation methods. While both studies consider shear-thinning fluids, in this research examines the influence of first-order slip conditions on MHD peristaltic flow,

offering insights into how slip at the boundaries affects flow in straight channels, a factor not considered by Akhtar et al.

Choudhari et al. [6] conducted a comprehensive study on the integration of electroosmotic and magnetohydrodynamic effects in peristaltic transport, with particular emphasis on physiological systems and biomedical applications. Their work highlights the synergy between electrokinetic and magnetic forces in enhancing flow control, providing a strong basis for optimizing fluid transport in microfluidic devices. Although their study encompasses electroosmotic and MHD effects, the present study focuses exclusively on the first-order slip condition in peristaltic transport of pseudoplastic fluids, with the aim of understanding its impact on pressure rate, velocity profiles, and frictional forces. This distinction allows our work to specifically address boundary-layer interactions in non-Newtonian flows under suction and injection effects, providing complementary insights into fluid dynamics in biomedical contexts.

Gudekote et al. [7] extended the study of peristaltic motion to non-Newtonian fluids in irregular channels, incorporating porous and convective boundary conditions. Their work addressed the impact of permeability and elasticity on fluid movement under peristaltic waves. In this research differs by focusing on first-order slip conditions rather than convective or porous boundaries. Additionally, while Gudekote et al. explored the effects of channel irregularity, we consider a symmetric channel with suction and injection, making our analysis more relevant to practical applications such as biomedical systems.

Goud et al. [8] investigated the influence of suction and injection on the peristaltic transport of pseudoplastic fluids between permeable boundaries. Their study used low Reynolds number and long wavelength assumptions, to simplify the governing equations. While both studies incorporate suction and injection. This research is different in addressing the slip condition's, MHD effects role in modulating velocity and pressure distributions, providing new insights into flow dynamics in channels with slip at the walls.

Rajashekhar et al. [9] examined the unsteady peristaltic flow of a Rabinowitsch fluid in a non-uniform channel, focusing on temperature-dependent viscosity and thermal conductivity. In this study diverges from this work by excluding temperature-dependent properties and focusing instead on the effects of slip and suction/injection. While Rajashekhar et al. analyze thermal effects, we provide a detailed investigation into velocity and pressure changes under slip conditions in pseudoplastic fluids.

Misra et al. [10] focused on the mechanics of fluid flow in biological systems, particularly in digestion and blood circulation, using non-Newtonian fluid models. They analyzed the role of peristalsis in fluid transport within biological channels. In this work builds on this by extending the non-Newtonian fluid analysis to pseudoplastic fluids with suction and injection, offering additional insights into industrial and biomedical systems where wall slip and suction/injection are critical factors.

Shah et al. [11] extends the understanding of Williamson fluid flow by incorporating bio-convection and magnetic field effects, using machine learning for fluid prediction and optimization. This study provides a detailed analysis of peristaltic transport in pseudoplastic fluids under slip, suction, and injection, offering analytical insights.

Geetha et al. [12] studies the non-Newtonian fluids and MHD effects, but they differ in fluid type (Williamson vs pseudoplastic), boundary conditions (peristaltic transport vs boundary layer flow), and focus (heat transfer vs pressure/velocity distributions). But this study is unique in its focus on peristaltic transport and slip conditions, while Geetha et al. deal with heat transfer and boundary layer effects in a porous medium.

Hasona et al. [13] explored the effects of varying thermal and electrical conductivity on pseudoplastic nanofluids in asymmetric, non-uniform channels. In this study, however, does not incorporate thermal and electrical conductivity variations but focuses on the influence of slip conditions and MHD effects on pseudoplastic fluid flow. This distinction marks a clear difference in the physical factors considered in both studies, with ours offering a more focused exploration of boundary conditions and fluid transport.

Rashid et al. [14] studied the peristaltic flow of Williamson fluid in a curved channel under an induced magnetic field. While they explored the Lorentz forces in the fluid dynamics, in this study does not specifically examine the Williamson fluid but instead focuses on pseudoplastic fluids under MHD conditions. Furthermore, our paper delves into the effects of first-order slip boundary conditions, a factor not examined in Rashid et al.'s work.

Moatimid et al. [15] expands the understanding of MHD flow instabilities in viscoelastic Bingham fluids, offering analytical insights into nonlinear stability mechanisms. The study focuses on the dynamics of peristaltic transport in pseudoplastic fluids, providing analytical solutions for practical scenarios involving suction, injection, and slip.

Babu et al. [16] investigated the effects of wall suction and injection on peristaltic flow in porous media. While they considered porous channels, the study looks at peristaltic transport with suction and injection effects in a straight channel, under MHD conditions, with a focus on first-order slip boundary conditions. The comparison is insightful as both studies examine flow modifications through boundary conditions, though in different geometries and fluid types.

Abbas et al. [17] examined the influence of wall injection and suction, Lorentz forces, and chemical reactions on the peristaltic flow of Jeffrey fluid. In paper focuses on a similar boundary condition setup (suction and injection) but specifically investigates the MHD peristaltic flow of pseudoplastic fluids under slip conditions, without considering chemical reactions. This difference in the scope of physical factors highlights our unique contribution to the field.

Kumar et al. [18] studied the effect of total slip on peristaltic flow in tapered channels, demonstrating the impact on velocity profiles and pressure distributions. While their work focuses on tapered geometries, our study uses a straight channel configuration, emphasizing how first-order slip conditions influence fluid transport in a simpler geometry. The slip conditions in both studies are similar, but the channel shape and flow characteristics differ.

Abbas et al. [19] examined MHD slip flow in a diverging tube, focusing on entropy production. Their study provides insights into how entropy generation is affected by magnetic fields and slip effects, while this paper focuses on peristaltic flow in a straight channel under MHD conditions with slip boundary conditions. While both studies explore entropy and flow efficiency, the geometries and fluid models differ, highlighting different aspects of flow dynamics.

Aman et al. [20] studied second-grade fluid flow under convective boundary conditions with suction and injection. Unlike Aman et al., who analyzed second-grade fluids, the study focuses on pseudoplastic fluids under MHD and slip conditions. This difference in fluid type and boundary condition setup contributes to a more specialized understanding of peristaltic flow under MHD conditions and slip effects.

A gap in the literature is filled by first simulating the physical solution and then addressing it with typical perturbation methods to obtain solutions that are analytical.

Peristaltic transport, characterized by wave-like contraction of the channel walls, is fundamental in applications such as gastrointestinal fluid flow, reproductive systems, and industrial transport mechanisms. This paper focuses on a specialized scenario involving pseudoplastic fluids, slipconditions, and magnetohydrodynamics (MHD), assuming a long wavelength and low Reynolds number flow.

1.1 *Pseudoplastic behavior*

Pseudoplastic fluids are Non-newtonian, meaning their flow properties differ from those of simple newtonian fluids like water. Specifically, Pseudoplastic fluid exhibit shear thinning behavior, where viscosity decreases as the shear rate increases. This behavior is common in biological fluids (eg., blood, synovial fluid) and industrial suspensions (eg., paints, polymer solutions) such properties are critical to understanding and predicting fluid motion in biomedical devices and industrial processes, as shear-thinning can significantly alter the velocity profile and energy requirements for flow.

1.2 *Slip condition*

The classical no-slip boundary condition assumes that the fluid at the wall moves with the wall's velocity, implying zero relative motion. However in many real-world systems, this assumption breaks down due to surface roughness, porous walls, or coatings (like lubricants or mucus). In such cases, the slip condition allows for partial movement of fluid at the boundary. This study incorporates the first-order partial slip condition, which quantitavely measures the relative slip between the fluid and the channel walls. Incorporating slip conditions is essential for analyzing flows in microscale and nanoscale systems, such as lab-on-chip devices or microfluidic channels, where boundary effects dominate.

1.3 *Magnetohydrodynamic (MHD) effects*

When an electrically conducting fluids moves through a maagnetic field, electromagnetic forces are generated. These forces influence the flow dynamics, either suppressing or enhancing motion depending onthe alignment of the magnetic field and the flow. In industrial processes. MHD effects are used for purposes such as controlling molten metal flow or stabilizing plasma in fusion reactors. In biomedical applications, magnetic fields are employed to stear magnetic nanoparticles or fluids for targeted drug delivery. This study examines how the magnetic field interacts with the pseudoplastic fluid flow under peristaltic motion, providing insights into scenarios where such control mechanisms are relevant.

1.4 *Physical relavance of the study*

By combining these phenomena-pseudoplastic behavior, partial slip conditions, and MHD effects. This study addresses the complexities of peristaltic transport in both natural and engineered systems. The analytical solution presented provides a framework for understanding how these parameters influence the velocity field, pressure difference, and frictional forces. The findings are graphically illustrated, highlighting the impact of Non-newtonian characteristics and boundary conditions on the system's overall performance.

This comprehensive approach allows for the exploration of scenanarios ranging from biological processes, such as nutrient transport in blood vessels, to engineering applications, such as nutrient transport in blood vessels, to engineering applications, such as chemical transport in micro reactors. The inclusion of slip and magnetic effects broadens the applicability of the study, making it valuable for designing efficient and controlled fluid transport systems.

2. Mathematical formulation

Consider the peristaltic transport of pseudoplastic fluid bounded by permeable walls of the channel width $2a$. The fluid is injected into the channel perpendicular to the lower permeable wall with a constant velocity (V_0) and is sucked out of the upper permeable wall with the same velocity (V_0) as shown in Figure 1. For simplicity, we restrict our discussion to the half width of the channel.

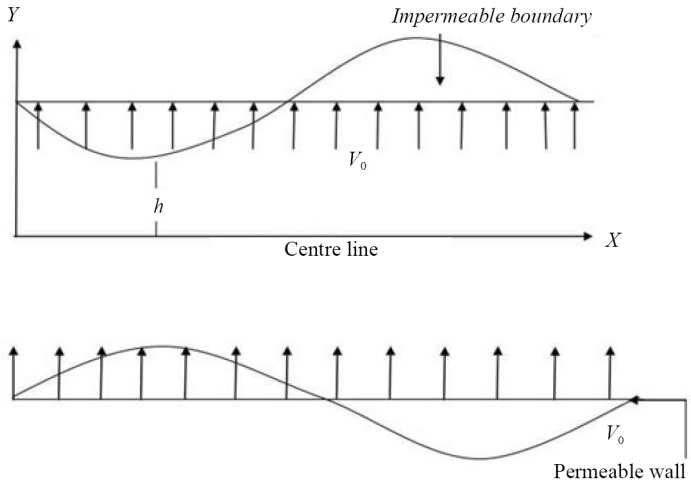

Figure 1. Physical model

The wall deformation is given by

$$Y = H(X,t) = a + b\cos\frac{2\Pi}{\lambda}(X - ct). \tag{1}$$

Here, λ represents the wavelength, c denotes a wave speed, and b refers to the amplitude.
The transformation from fixed frame to wave frame are introduced as follows:

$$u = U - c,\ y = Y,\ x = X - ct,\ p(x,y) = P(X,Y,t),\ v_0 = V_0.$$

In order to write the governing equations and the boundary conditions in dimensionless form, the following non-dimensional quantities are introduced by Goud and Reddy [8].

$$\bar{u} = \frac{u}{c},\ \bar{x} = \frac{x}{\lambda},\ \bar{y} = \frac{y}{a},\ \bar{v_0} = \frac{v_0}{c},\ \delta = \frac{a}{\lambda},\ \bar{t} = \frac{ct}{\lambda},\ \bar{p} = \frac{a^2 p}{\mu c\lambda},\ \bar{pi} = \frac{b}{a},\ Re = \frac{ca\rho}{\mu},\ \mu_1 = \frac{\mu_1 c}{a},$$

$$\bar{S_{ij}} = \frac{aS_{ij}}{\mu c}\ (\text{for } i,\ j = 1, 2, 3, ...),\ \lambda_1 = \frac{\lambda_1 c}{a},\ \bar{\alpha} = \frac{\alpha}{a},\ u = \frac{\partial\psi}{\partial y},\ v = -\delta\frac{\partial\psi}{\partial y},\ M = \sqrt{\frac{\sigma c}{\mu}}B_0 a.$$

δ denotes the wave amplitude, ψ the stream function, and Re the Reynolds number, non-dimensional relaxation times by λ_1 and μ_1, and the slip parameter by α.

Under the assumptions of long wavelength and low Reynolds number (after dropping bars), we get

$$\frac{\partial p}{\partial x} = \frac{\partial S_{xy}}{\partial y} - k\frac{\partial u}{\partial y} - M^2(u+1). \tag{2}$$

$$\frac{\partial p}{\partial y} = 0. \tag{3}$$

Here

$$k = Re.v_0, \tag{4}$$

$$S_{xx} = (\lambda_1 + \mu_1)S_{xy}\left(\frac{\partial u}{\partial y}\right).$$

$$S_{yy} = (-\lambda_1 + \mu_1)S_{xy}\left(\frac{\partial u}{\partial y}\right).$$

$$S_{xy} = \frac{\dfrac{\partial u}{\partial y}}{1 + \Gamma\left(\dfrac{\partial u}{\partial y}\right)^2}. \tag{5}$$

The corresponding dimensionless boundary conditions in wave frame of reference are given by

$$\frac{\partial u}{\partial y} = 0 \text{ at } y = 0. \tag{6}$$

$$u = -1 - \alpha \frac{\partial u}{\partial y} \text{ at } y = h = 1 + \phi cos2\pi x. \tag{7}$$

The volume flow rate q in a wave frame of reference is given by

$$q = \int_0^{h(x)} u dy. \tag{8}$$

The instantaneous flux $Q(X, t)$ in a fixed frame is.

$$Q(X, t) = \int_0^h U dY = \int_0^h (u + 1) dy = q + h. \tag{9}$$

The time average flux $\bar{Q}$ over one period T (where $T = \frac{\lambda}{c}$) of the peristaltic wave is defined by

$$\bar{Q} = \frac{1}{T} \int_0^T Q dt = \int_0^1 (q + h) dx = q + 1. \tag{10}$$

3. Analytically solved by using perturbation method

The equation (4) is non-linear. We linearize this equation in terms of Γ, the small relaxation parameter for the flow. So we expand u, p and q as

$$u = u_0 + \Gamma u_1 + O(\Gamma^2)$$

$$p = p_0 + \Gamma p_1 + O(\Gamma^2)$$

$$q = q_0 + \Gamma q_1 + O(\Gamma^2). \tag{11}$$

Substituting (11) in the equation (2) and in the boundary conditions (6) and (7) and equating the coefficient of like powers of Γ to zero and neglecting the of Γ^2 and higher order, we get the following equations.

Equation of order Γ^0

$$\frac{dp_0}{dx} = \frac{\partial^2 u_0}{\partial y^2} - k \frac{\partial u_0}{\partial y} - M^2 (u_0 + 1). \tag{12}$$

and the respective boundary conditions are

$$\frac{\partial u_0}{\partial y} = 0, \quad \text{at } y = 0. \tag{13}$$

$$u_0 = -1 - \alpha \frac{\partial u_0}{\partial y}, \quad \text{at } y = h. \tag{14}$$

Using boundary conditions (13) and (14) to solve equation (12) yields the velocity equation.

$$u_0 = -1 + \left[\frac{P_0}{M^2}\right]\left[\frac{e^{c_1 y}}{k_1} + \frac{e^{c_2 y}}{k_2} - 1\right]. \tag{15}$$

Here

$$c_1 = \frac{k + \sqrt{k^2 + 4M^2}}{2},$$

$$c_2 = \frac{k - \sqrt{k^2 + 4M^2}}{2}.$$

$$k_1 = e^{c_1 h}[1 + \alpha c_1] - \frac{c_1}{c_2} e^{c_2 h}[1 + \alpha c_2].$$

$$k_2 = e^{c_2 h}[1 + \alpha c_2] - \frac{c_2}{c_1} e^{c_1 h}[1 + \alpha c_1].$$

The volume flux q_0 is given by

$$q_0 = \int_0^h u_0 dy = -h + \left[\frac{P_0}{M^2}\right]\left[\frac{e^{c_1 h} - 1}{k_1 c_1} + \frac{e^{c_2 h} - 1}{k_2 c_2} - h\right]. \tag{16}$$

From equation (16) we have $p_0 = \dfrac{dp_0}{dx}$.

$$\frac{dp_0}{dx} = P_0 = \frac{M^2(q_0)}{k_3} + h \tag{17}$$

Here

$$K_3 = \left[\frac{e^{c_1 h} - 1}{k_1 c_1} + \frac{e^{c_2 h} - 1}{k_2 c_2} - h\right]$$

Equation of order Γ^1

$$\frac{dp_1}{dx} = \frac{\partial^2 u_1}{\partial y^2} - \frac{\partial}{\partial y}\left[\frac{\partial u_0}{\partial y}^3\right] - k\frac{\partial u_1}{\partial y} - M^2(u_1+1) \tag{18}$$

and the respective boundary conditions are

$$\frac{\partial u_0}{\partial y} = 0, \quad \text{at } y = 0. \tag{19}$$

$$u_0 = -1 - \alpha\frac{\partial u_0}{\partial y}, \quad \text{at } y = h. \tag{20}$$

Evaluating equation (18) with boundary conditions (19) and (20) results in a velocity equation.

$$u_1 = \left[-\frac{P_1}{M^2} - 1\right]\left[\frac{e^{c_1 y}}{k_1} + \frac{e^{c_2 y}}{k_2} - 1\right] + \left[\frac{P_0}{M^2}\right]^3 k_{17}\left[\frac{e^{c_1 y}}{k_1} + \frac{e^{c_2 y}}{k_2}\right]$$

$$-\left[\frac{P_0}{M^2}\right]^3 k_{12}e^{c_1 y} + \left[\frac{P_0}{M^2}\right]^3 \left[(3k_4)k_5 e^{3c_1 y} + (3k_6)k_7 e^{3c_2 y} + (3k_8)k_9 e^{2c_1 y e^{c_2 y}} + (3K_{10})k_{11}e^{c_1 y}e^{2c_2 y}\right]$$

Here,

$$k_4 = \frac{c_1^4}{k_1^3}$$

$$k_5 = \frac{1}{3(3c_1^2 - kc_1 - (1/3)(M^2))}$$

$$k_6 = \frac{c_2^4}{k_2^3}$$

$$k_7 = \frac{1}{3(3c_2^2 - kc_2 - (1/3)(M^2))}$$

$$k_8 = \frac{c_1^2 c_2(2c_1 + c_2)}{k_1^2 k_2}$$

$$k_9 = \frac{1}{(2c_1+c_2)^2 - k(2c_1+c_2) - M^2}$$

$$k_{10} = \frac{c_1 c_2^2 (c_1+2c_2)}{k_1 k_2^2}$$

$$k_{11} = \frac{1}{(c_1+2c_2)^2 - k(c_1+2c_2) - M^2}$$

$$k_{12} = 3(3k_4)k_5 + 3(3k_6)k_7\frac{c_2}{c_1} + 2(3k_8)k_9 c_2 + 2(3k_{10})k_{11}c_2$$

$$k_{13} = [1+\alpha c_1]$$

$$k_{14} = [1+\alpha 3c_1]$$

$$k_{15} = [1+\alpha 3c_2]$$

$$k_{16} = [1+\alpha 2c_1 c_2]$$

$$k_{17} = k_{12}k_{13}e^{c_1 h} - (3k_4)k_5 k_{14}e^{3c_1 h} - (3k_6)k_7 k_{15}e^{3c_2 h}$$
$$- (3k_8)k_9 k_{16}e^{2c_1 h}e^{c_2 h} - (3k_{10})k_{11}k_{16}e^{c_1 h}e^{2c_2 h}$$

The volume flux through each cross-section is given by

$$q_1 = \int_0^h u_1 dy = \left[-\frac{P_1}{M^2} - 1\right]k_3 + \left[\frac{P_0}{M^2}\right]^3 [k_{18} - k_{19} + k_{20}]. \tag{21}$$

Then,

$$k_{18} = k_{17}\left[\frac{e^{c_1 h}-1}{k_1 c_1} + \frac{e^{c_2 h}-1}{k_2 c_2}\right]$$

$$k_{19} = k_{12}\left[\frac{e^{c_1 h}-1}{k_1 c_1}\right]$$

$$k_{20} = (3k_4)k_5\frac{e^{3c_1 h}-1}{3c_1} + (3k_6)k_7\frac{e^{3c_2 h}-1}{3c_2} + (3k_8)k_9\frac{e^{2c_1 h}-1}{2c_1}\frac{e^{c_2 h}-1}{c_2} + (3k_{10})k_{11}\frac{e^{c_1 h}-1}{c_1}\frac{e^{2c_1 h}-1}{2c_2}$$

From equation (21) we have

$$\frac{dp_1}{dx} = P_1 = -\frac{q_1}{k_3}M^2 - 1 + \left[\frac{P_0}{M^2}\right]^3 [k_{18} - k_{19} + k_{20}]. \tag{22}$$

Substitute equation (17) and (22) in equation (11) and using the relation

$$\frac{dp_0}{dx} = \frac{dp}{dx} - \Gamma\frac{dp_1}{dx}$$

And neglecting greater than $0(\Gamma^2)$ terms we get

$$u = -1 + \left[\frac{P}{M^2}\right]\left[\frac{e^{c_1 y}}{k_1} + \frac{e^{c_2 y}}{k_2} - 1\right] + \Gamma\left[\frac{P}{M^2}\right]^3 k_{17}\left[\frac{e^{c_1 y}}{k_1} + \frac{e^{c_2 y}}{k_2}\right] - \left[\frac{P}{M^2}\right]^3 k_{12}e^{c_1 y}$$

$$+\Gamma\left[\frac{P}{M^2}\right]^3 \left[(3k_4)k_5 e^{3c_1 y} + (3k_6)k_7 e^{3c_2 y} + (3k_8)k_9 e^{2c_1 y e^{c_2 y}} + (3K_{10})k_{11}e^{c_1}ye^{2c_2 y}\right]$$

Similarly,

$$\frac{dp}{dx} = M^2\frac{(q+h)}{k_3} + 1 + \Gamma[(q+h)]^3\frac{[k_{18} - k_{19} + k_{20}]}{(k_3)^3}. \tag{23}$$

In a wave frame, the dimensionless pressure increase and frictional force are

$$\Delta P = \int_0^1 \frac{dp}{dx}dx. \tag{24}$$

$$F = \int_0^1 h(-\frac{dp}{dx})dx. \tag{25}$$

4. Result and discussion

We disscused the variation for the graph are shown by using MATLAB Software. In Figure 2 demonstrates that magnetic parameter M represents the strength of the magnetic field in the governing equations. When the magnetic field is strong (M is high), the fluid experiences a braking effect due to electromagnetic drag. This is especially significant in conducting fluids (e.g., MHD flows). Increasing the magnetic parameter M increased the velocity profile. The propogation field is impacted by the current produced by the movement of conductive fluids across the magnetic field. On the other side, a body force known as the lorentz force, which affects fluid flow, is connected to the flow of an electric current through a magnetic field. Figure 3 the parameter k represents suction and injection at the channel walls. Stronger suction and injection increases the flow rate, enhancing the velocity profile. As k increases, the velocity magnitudes across the channel increases. The velocity profile is calculated based on k, which affects leading to a steeper or more enhanced profile for higher k. With increasing k, the velocity curve shifts upward, showing higher velocity magnitudes. Suction

and injection has practical applications in controlling fluid flow in medical devices, industrial channels, or heat exchangers. This simulation helps visualize how adjusting k changes the velocity distribution.

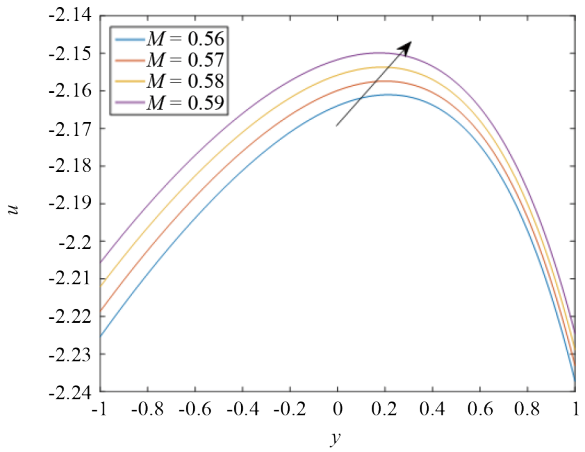

Figure 2. The variation in velocity for various M with $\phi = 0.33$, $\alpha = 0.15$, $\Gamma = 0.51$, $k = 0.28$

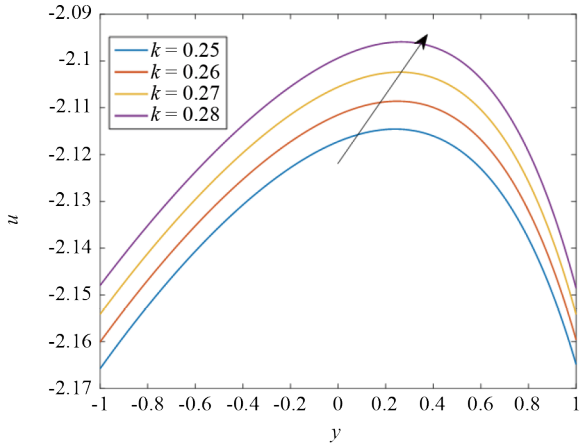

Figure 3. The variation in velocity for various k with $M = 0.58$, $\Gamma = 0.45$, $\alpha = 0.28$, $\phi = 0.75$

From Figure 4 it has shown that as Γ increases, it reflects an enhancement in nonlinearity, boundary perturbations, or fluid property changes. The effects of increasing Γ can be linked to velocity profile enhancement, a higher Γ amplifies the impact of nonlinearity, leading to more pronounced velocity distributions. A higher Γ typically leads to increased velocity near the center of the channel. Greater deviation in the velocity profile, showcasing enhanced transport capability, reduced maximum pressure at the boundaries, which can lower energy consumption in fluid systems for pseudoplastic fluids ($\Gamma > 0$), increasing Γ reflects stronger pseudoplastic behavior, leading to more complex flow characteristics. In real world application peristalsis is influenced by the perturbation parameter Γ, especially for biological fluids (eg.: mucus or chyme). Increasing Γ ensures efficient fluid transport and mixing, critical for drug delivery, artificial pumps, and diagnostics. From Figure 5 as α increases, the velocity distribution within the channel becomes more prominent. This is because the fluid's movement is heavily influenced by the wave-induced motion. The maximum velocity increases near the centre of the channel, while near the boundaries, the flow may experience higher shearing effects. In real world application it is used in biomedical system in artificial organs (eg., heart-lung machines or dialysis pumps), increasing α ensures stronger pumping, mimicking the natural motion of biological organs. Higher α values represent stronger

peristaltic contractions, improving food transport in the intestines or aiding in the study of digestive disorders. From Figure 6 the amplitude ratio ϕ is a key parameter in the study of peristaltic or wave-induced flow. When ϕ increases, Enhanced peristaltic action the oscillations of the channel walls become more pronounced leading to stronger compression and expansion of the fluid. The increase in ϕ amplifies the net forward motion of the fluid, enhancing the efficiency of peristaltic pumping. This is beneficial for transporting fluids, especially in low reynolds number regimes or in viscous fluid. In real world application artificial pumps in devices like blood pumps or dialysis machines, increasing ϕ enhances the pumping efficiency, mimicking natural peristalsis. Larger ϕ values can be used to optimize drug transport in systems involving oscillatory motion or peristaltic mechanisms.

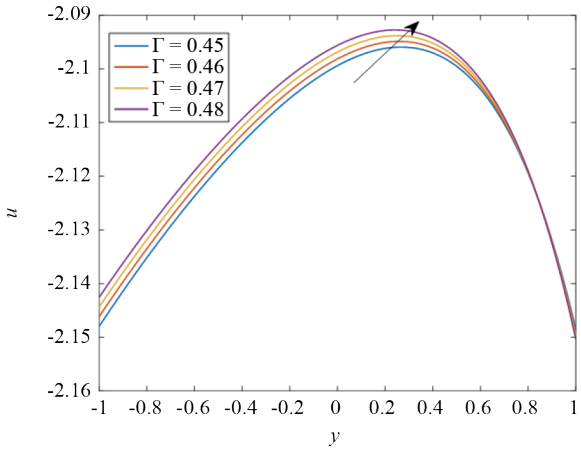

Figure 4. The variation in velocity for various Γ with $M = 0.58$, $k = 0.28$, $\alpha = 0.28$, $\phi = 0.75$

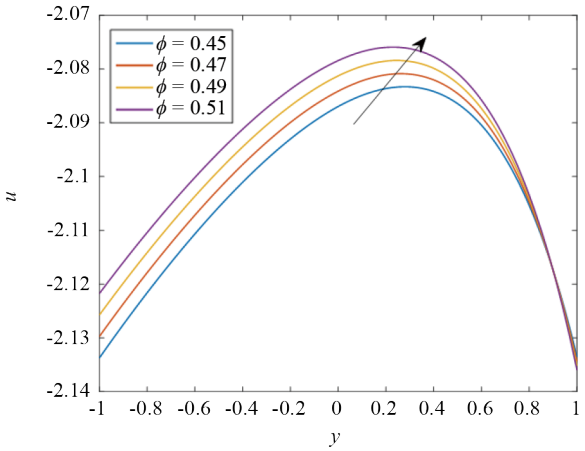

Figure 5. The variation in velocity for various ϕ with $\Gamma = 0.35$, $M = 0.61$, $k = 0.71$, $\alpha = 0.25$

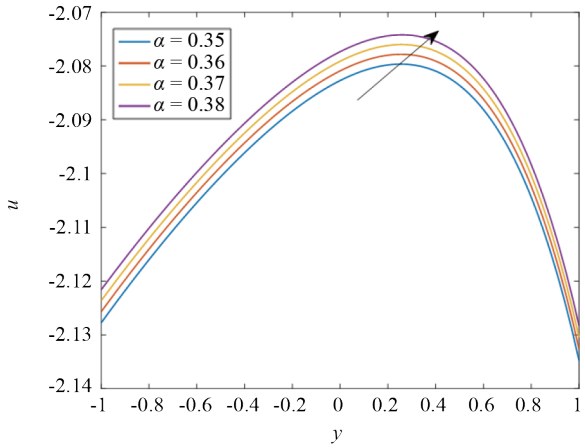

Figure 6. The variation in velocity for various α with $M = 0.58$, $k = 0.28$, $\Gamma = 0.45$, $\phi = 0.75$

From Figure 7 with increasing M, the magnetic field dampens the fluid motion, reduces velocity, and increases viscosity, which collectively results in a decrease in pressure value. The pressure rate fluctation for various values of suction and injection parameter k is shown in Figure 8. It has been observed that while the value k is increased but the pressure rate is decreased. As the perturbation parameter increases, the pumping rate tends to increase as well, as shown in Figure 9. This suggests that during peristalsis, a pseudoplastic fluid experiences a greater pressure rise than a viscous fluid. From the Figure 10 it has shown that pressure rate increases as the values of the amplitude ratio ϕ decreases. From Figure 11 shows the variation in the slip value decreases the pressure rate. This means that the fluid slippage at the wall reduces the maximum pressure against which the peristalsis works as a pump. From Figure 12-16 represents the frictional force is just behavior to the pressure rate.

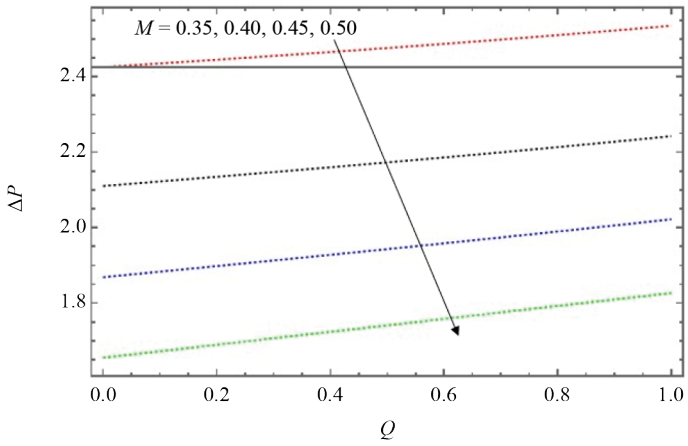

Figure 7. The difference of Δp with Q for various M with $\phi = 0.4$, $\alpha = 0.20$, $k = 0.30$, $\Gamma = 0.01$

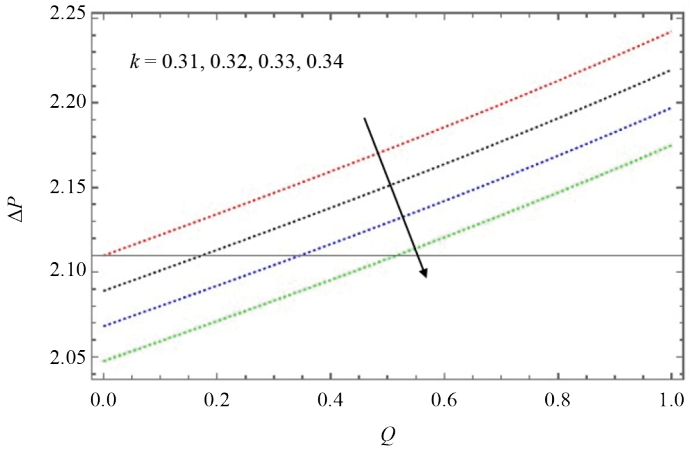

Figure 8. The difference of Δp with Q for various Γ with $\phi = 0.4$, $\alpha = 0.20$, $k = 0.30$, $\Gamma = 0.01$, $M = 0.4$

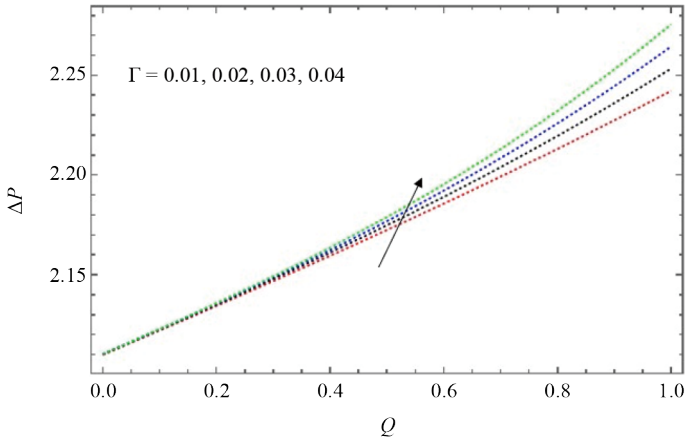

Figure 9. The difference of Δp with Q for various k with $\phi = 0.4$, $\alpha = 0.20$, $k = 0.45$, $\Gamma = 0.01$, $M = 0.4$

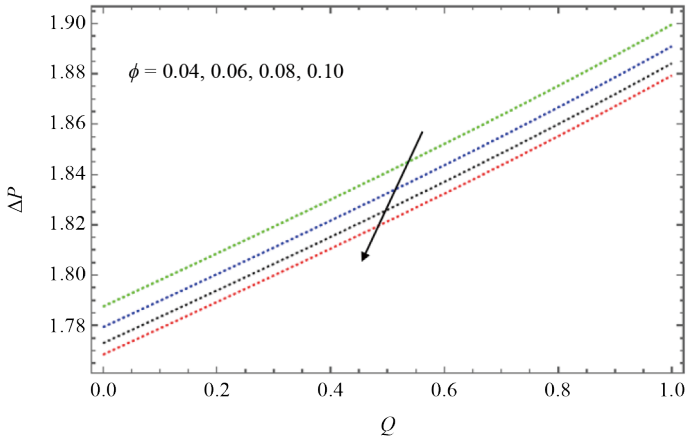

Figure 10. The difference of Δp with Q for various ϕ with $\alpha = 0.4$, $k = 0.3$, $\Gamma = 0.01$, $M = 0.4$

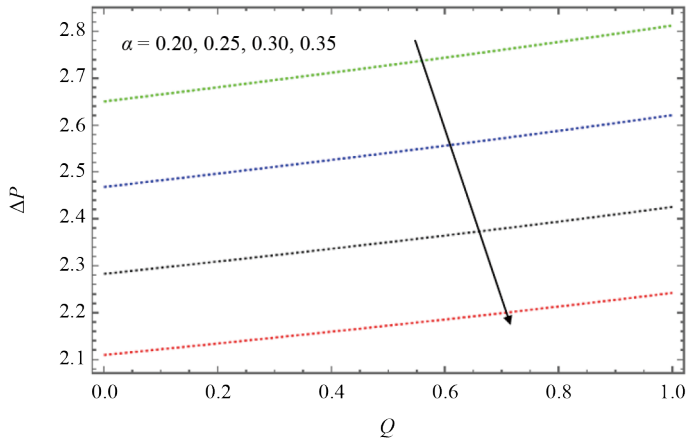

Figure 11. The difference of Δp with Q for various α with $\phi = 0.4$, $k = 0.3$, $\Gamma = 0.01$, $M = 0.4$

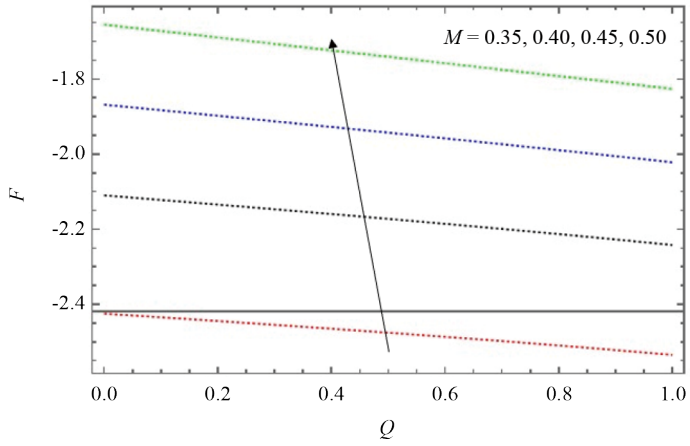

Figure 12. The difference of F with Q for various M with $\phi = 0.4$, $\alpha = 0.20$, $k = 0.30$, $\Gamma = 0.01$

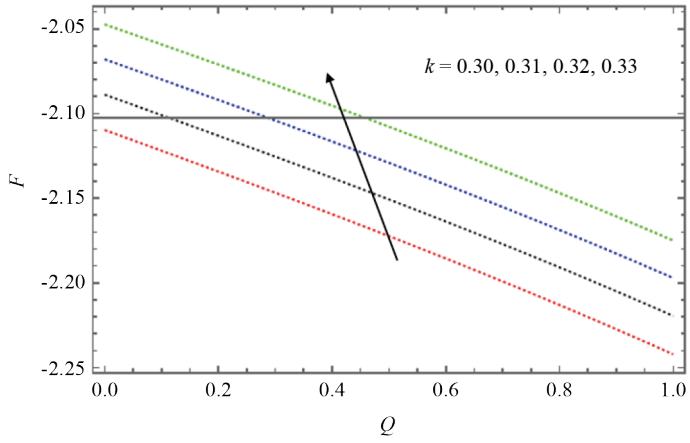

Figure 13. The difference of F with Q for various k with $\phi = 0.4$, $\alpha = 0.20$, $\Gamma = 0.01$, $M = 0.4$

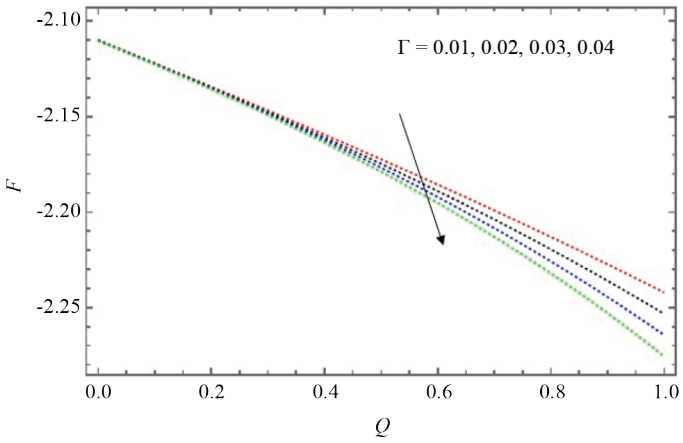

Figure 14. The difference of F with Q for various Γ with $\phi = 0.4$, $\alpha = 0.20$, $k = 0.30$, $\Gamma = 0.01$, $M = 0.4$

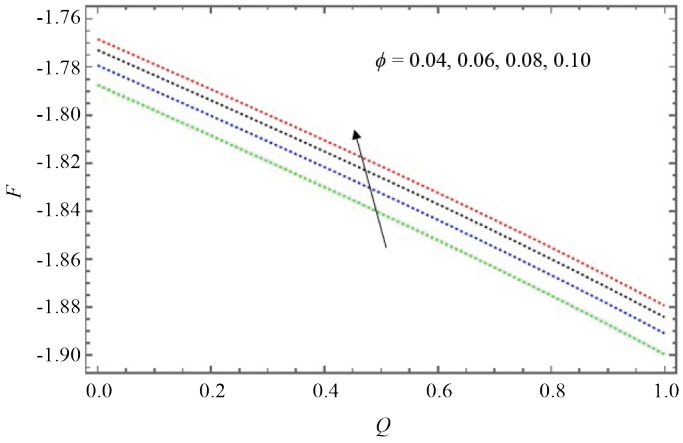

Figure 15. The difference of Δp with Q for various ϕ with $\alpha = 0.4$, $k = 0.3$, $\Gamma = 0.01$, $M = 0.4$

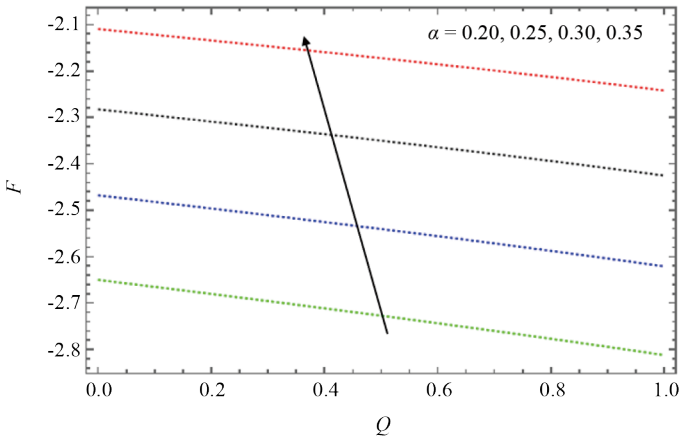

Figure 16. The difference of Δp with Q for various α with $\phi = 0.4$, $k = 0.3$, $\Gamma = 0.01$, $M = 0.4$

5. Conclusion

The peristaltic motion of magnetohydrodynamic (MHD) pseudoplastic fluids in the presence of injection and suction is investigated in this work, assuming a tiny Reynolds number with a long wavelength. Using perturbation techniques to evaluate the analytical solution and the expression for the velocity, pressure gradient and frictional force are derieved. It seems that perturbation solution can provide a good approximation for small perturbation parameters. Various physical characteristics effects on pressure rate, pressure gradient, velocity and frictional force is graphically explained for various values of Non-newtonian and slip effects.

1) In the velocity profile increasing the value of suction and injection parameter k. M, α, ϕ, Γ values. It show that the value of strong magnetic field increases and then the suction and injection parameter, perturbation parameter is also increases. The magnitude of the pressure gradient in viscous fluid is smaller than pseudoplastic.

2) The pressure gradient value is increased in Γ, and then decreased in the remaining parameters.

3) The frictional force is just opposite behavior for the pressure gradient.

6. Application

The analysis of pseudoplastic liquid peristaltic transport in the context of a first-order partial slip condition, combined with MHD effects, and confined by permeable walls with suction and injection has significant implications for both biological and industrial processes. In biomedical domains, this research is critical for understanding and optimising fluid flow in many physiological systems, including the gastrointestinal tract, blood circulation, and lymphatic systems, where non-Newtonian fluids like mucus and blood exhibit pseudoplastic behaviour. The use of first-order slip conditions and magnetic fields enables a more precise simulation of microfluidic flows in devices like as pumps and catheters, which are used for drug administration and other therapeutic interventions. The findings of this study can be applied in industrial processes such as polymer extrusion, food processing, and chemical engineering, all of which involve pseudoplastic fluids. Controlling peristaltic transport via porous walls using suction and injection boosts filtration system efficiency, material mixing, and heat or mass transfer processes. The magnetic field, along with slip conditions, influences flow behaviour in electromagnetic pumps and reactors, allowing for precise control over fluid dynamics in production settings. Consequently, our work significantly enhances industrial processes requiring complicated fluid flows as well as biomedical equipment. Since magnetohydrodynamics (MHD) links the action of magnetic fields to the behavior of electrically conducting fluids, it is pertinent to our discussion. The MHD effect is important in this study because it enables the manipulation and control of fluid flow by combining electromagnetic forces with fluid motion. MHD is a non-invasive method of controlling fluid movement in biological systems, such as blood flow and drug delivery systems, that does not require physical contact. Blood, as a conducting fluid due to its ion content, can be affected by an external magnetic field. This enables control over flow rates and patterns in microfluidic devices used for focused medicine administration, dialysis, and other medical applications. MHD can either increase or decrease peristaltic movements, depending on the therapeutic need, which can be critical in controlling drug flow or guiding particles through the bloodstream.

Author contribution

All authors have contributed equally to the development of this paper.

Conflict of interest

The authors declare no competing financial interest.

References

[1] Ali HA, Salman MR. Influence of rotation on peristaltic flow for pseudoplastic fluid: a wavy channel. *An International Journal of Optimization and Control: Theories and Applications (IJOCTA)*. 2024; 14(4): 336-345.

[2] Ramesh K, Devakar M. Magnetohydrodynamic peristaltic flow of Pseudoplastic fluid in a vertical asymmetric channel through porous medium with heat and mass transfer. *Iranian Journal of Science and Technology, Transactions A: Science*. 2017; 41: 257-272.

[3] Noreen S, Zahra M, Lu DC. Pseudoplastic fluid flow via electroosmotic and peristaltic pumping. *Waves in Random and Complex Media*. 2022; 1-21.

[4] Jayavel P, Jhorar R, Tripathi D, Azese MN. Electroosmotic flow of pseudoplastic nanoliquids via peristaltic pumping. *Journal of the Brazilian Society of Mechanical Sciences and Engineering*. 2019; 41(2): 61.

[5] Akhtar S, Shahzad MH, Nadeem S, Awan AU, Almutairi S, Ghazwani HA, et al. Analytical solutions of PDEs by unique polynomials for peristaltic flow of heated Rabinowitsch fluid through an elliptic duct. *Scientific Reports*. 2022; 12(1): 12943.

[6] Choudhari R, Tripathi D, Vaidya H, Prasad KV, Shetty J, Mebarek-Oudina F, et al. Integrated analysis of electroosmotic and magnetohydrodynamic peristaltic pumping in physiological systems: Implications for biomedical applications. *ZAMM-Journal of Applied Mathematics and Mechanics/Zeitschrift für Angewandte Mathematik und Mechanik.* 2024; e202400163.

[7] Gudekote M, Vaidya H, Baliga D, Choudhari R, Prasad KV. The effects of convective and porous conditions on peristaltic transport of non-Newtonian fluid through a non-uniform channel with wall properties. *Journal of Advanced Research in Fluid Mechanics and Thermal Sciences*. 2019; 63(1): 52-71.

[8] Goud JS, Reddy RH. Peristaltic transport of a pseudoplastic fluid bounded by permeable walls with suction and injection. *International Journal of Pure and Applied Mathematics*. 2017; 113(6): 289-297.

[9] Rajashekhar C, Vaidya H, Prasad KV, Tlili I, Patil A, Nagathan P. Unsteady flow of Rabinowitsch fluid peristaltic transport in a non-uniform channel with temperature-dependent properties. *Alexandria Engineering Journal*. 2020; 59(6): 4745-4758.

[10] Misra JC, Pandey SK. Peristaltic transport of physiological fluids. In: *Biomathematics: Modelling and Simulation*. Singapore: World Scientific; 2006. p.167-193.

[11] Priyadharshini P, Karpagam V, Shah NA, Alshehri MH. Bio-convection effects of MHD williamson fluid flow over a symmetrically stretching sheet: machine learning. *Symmetry*. 2023; 15(9): 1684.

[12] Geetha R, Reddappa B, Tarakaramu N, Rushi Kumar B, Ijaz Khan M. Effect of double stratification on MHD Williamson boundary layer flow and heat transfer across a shrinking/stretching sheet immersed in a porous medium. *International Journal of Chemical Engineering*. 2024; 2024(1): 9983489.

[13] Hasona WM, Almalki NH, ElShekhipy AA, Ibrahim MG. Combined effects of variable thermal conductivity and electrical conductivity on peristaltic flow of pseudoplastic nanofluid in an inclined non-uniform asymmetric channel: applications to solar collectors. *Journal of Thermal Science and Engineering Applications*. 2020; 12(2): 021018.

[14] Rashid M, Ansar K, Nadeem S. Effects of induced magnetic field for peristaltic flow of Williamson fluid in a curved channel. *Physica A: Statistical Mechanics and its Applications*. 2020; 553: 123979.

[15] Moatimid GM, Mohamed YM. Novel analytical perspectives on nonlinear instabilities of viscoelastic Bingham fluids in MHD flow fields. *Scientific Reports*. 2024; 14(1): 28843.

[16] Babu VR, Sreenadh S, Srinivas AN. Peristaltic transport of a viscous fluid in a porous channel with suction and injection. *Ain Shams Engineering Journal*. 2018; 9(4): 909-915.

[17] Abbas Z, Rafiq MY, Hasnain J, Umer H. Impacts of lorentz force and chemical reaction on peristaltic transport of Jeffrey fluid in a penetrable channel with injection/suction at walls. *Alexandria Engineering Journal*. 2021; 60(1): 1113-1122.

[18] Kumar PR, Babu VR. Effect of complete slip on peristaltic transport of Jeffrey fluid flow in a tappered channel with suction and junction. *International Journal of Mechanical Engineering and Technology*. 2019; 10(2): 551-560.

[19] Abbas Z, Rafiq MY, Alshomrani AS, Ullah MZ. Analysis of entropy generation on peristaltic phenomena of MHD slip flow of viscous fluid in a diverging tube. *Case Studies in Thermal Engineering*. 2021; 23: 100817.

[20] Aman S, Ismail Z, Salleh MZ, Khan I. Flow analysis of second grade fluid with wall suction/injection and convective boundary condition. *Journal of Advanced Research in Fluid Mechanics and Thermal Sciences*. 2019; 58(1): 135-143.